Journal of Thermal Analysis, Vol. 32 (1987) 1209–1218

SPECTRAL PROPERTIES AND TEMPERATURE-DEPENDENCE OF SEMICONDUCTIVITY OF VARIOUS DOPED BISMUTH TRIOXIDE POLYCRYSTALS

*M. M. Abou Sekkina** and *E. El-Shereafy***

*FACULTY OF SCIENCE, TANTA UNIVERSITY, TANTA, EGYPT
**FACULTY OF SCIENCE, EL-MONOUFEIA UNIVERSITY, SHIBIN EL-KOM, EGYPT

(Received September 7, 1985; in revised form November 5, 1986)

Several samples of Nb_2O_5-doped Bi_2O_3 and Y_2O_3-doped Bi_2O_3 were carefully prepared and sintered at 700° for 3 hours. Extensive measurements were carried out on these samples, including X-ray diffraction spectra, infrared absorption spectra and the temperature-dependence of the DC-electrical conductivity in the solid state. The results obtained were discussed, correlated and interpreted. Finally, the optimum compositions were established and recommended for doped-Bi_2O_3 in the electronics industry.

The interest in the spectral and semiconducting properties of various doped polycrystals is due to the use of Bi_2O_3 as a sintering aid for the preparation of ZnO high-field varistors. A varistor is a variable resistor in that its resistance decreases rapidly with increasing voltage above a threshold value [1, 2]. Since this breakdown voltage is strongly dependent on grain size, it is important to limit the size of the ZnO grains for a high-field device. Varistors are usually prepared from a mixture of metal oxides such as ZnO, CoO, Bi_2O_3 and PbO.

Although several theories have been proposed to explain the effects of certain oxides on the properties of varistors, their roles are not completely understood or characterized. While it is thought that Bi_2O_3 does not affect the electrical properties of the ZnO grains themselves, it has been postulated that Bi_2O_3 affects the electrical properties of the grain boundaries of the varistors [1–4].

Bismuth sesquioxide (Bi_2O_3) has four polymorphic forms: a monoclinic α-form stable below 730°, a cubic γ-form stable above 730° to the melting point (825°), a metastable tetragonal β-form, and a bcc γ-form which appears during cooling of the γ-form. It has been reported that the γ-form has a deficient fluorite structure, with

* Author to whom all correspondence should be addressed; Present address: Faculty of Science, The United Arab Emirates University, Al-Ain, P.O. box 15551 (U.A.E.).

John Wiley & Sons, Limited, Chichester
Akadémiai Kiadó, Budapest

two vacant oxygen sites in a unit cell [5–8], and shows a high oxygen ion conductivity, which is more than one order of magnitude higher than that of stabilized zirconia. Whereas the monoclinic form displays low electronic conductivity [9], the pure β-form has been reported to exhibit an ionic and electronic mixed conduction, where the electronic conduction is predominant below a partial oxygen pressure PO_2 of 10 Pa [10]. The frequency dispersion of impedance reported by Harving and General [9] also suggests ionic conduction in the pure β-form in air.

As concerns the doped β-form, high ionic transference numbers of more than 85% for the systems Bi_2O_3–Y_2O_3 and Bi_2O_3–MoO_3 at high PO_2 were reported by Takahashi et al. [11, 12]. However, the conduction mechanism in the doped β-form still remains obscure.

Thus, the objective of the present investigation is to correlate the spectral properties of various doped Bi_2O_3 specimens with their semiconducting parameters, in an attempt to evaluate the optimum compositions for their useful application in the synthesis of varistors in industry.

Experimental

Sample preparation: The starting materials were Bi_2O_3 (99.99%), particle size 5–7 μm; Nb_2O_5 (99.98%) and Y_2O_3 (99.96%). Powder samples containing pure Bi_2O_3 and 2–10 mol % of either Nb_2O_5 or Y_2O_5 were carefully mixed, finely ground and pressed into pellets of about 10 μm diameter and 2 mm thickness. The pressed pellets were sintered at 700° for 3 hours in air and then furnace-cooled to room temperature.

X-ray diffraction measurements (XRD): The polymorphic forms of Bi_2O_3 were determined using a Shimadzu (Japan) X-ray diffractometer. Cu K_α radiation and an adjustable slit at the focal point of the monochromator were used. A Geiger–Müller tube was adjusted at a rate of one degree per minute. The diffraction patterns were recorded automatically at room temperature in the range $2\theta = 10°$ to 80°.

Infrared absorption measurements: The room-temperature IR absorption spectra were recorded using the potassium bromide disk technique. A Perkin–Elmer infrared spectrophotometer (Chart No. 5100 4366) was used in the range 4000–200 cm^{-1}.

DC-electrical conductivity measurements: The DC-electrical conductivity was measured as described previously by Abou-Sekkina et al. [13] with some modifications. Pellets about 10 mm in diameter and 2 mm in thickness were used as specimens for electrical conductivity measurements. Gold was evaporated onto the faces of the specimen to form a guarded electrode system which consisted of a main electrode 1.2 cm in diameter, a ring-shaped guarded electrode and an electrode

opposite. The measurements were carried out in a vertical wire-wound tube furnace, with the windings running in opposite directions to eliminate fields caused by the heating current. A 616 β-Keithley electrometer (U.S.A.) was utilized, and the circuit used was well shielded with copper. Measurements were made at room and elevated temperatures up to 500 K, and readings were taken 15 minutes after each temperature equilibration.

In all of the above measurements, the readings were taken three times and in each case good reproducible data were obtained.

Results and discussion

Figure 1 shows the room-temperature KBr absorption spectra of pure and various Nb_2O_5-doped Bi_2O_3 samples. Figure 2 gives the corresponding data for Y_2O_3-doped Bi_2O_3. Table 1 lists the main characteristic IR absorption bands and their corresponding energies in eV for both Nb_2O_5 and Y_2O_3-doped Bi_2O_3.

From Figs 1 and 2, the clusters of relatively narrow bands in the range 400–650 cm^{-1} in the IR spectra could be correlated with the stretching vibrations of various Bi—O bonds [14]. These clusters are obviously found more in the case of Nb_2O_5-doped Bi_2O_3 samples than Y_2O_3-doped ones; this is most probably

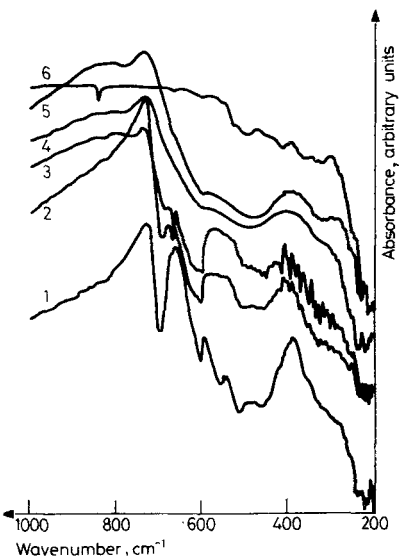

Fig. 1 A figure showing the infrared spectra of pure and Nb_2O_5-doped Bi_2O_3 samples. 1.– 2 mol % Nb_2O_5; 2.– 4 mol % Nb_2O_5; 3.– 5 mol % Nb_2O_5; 4.– 8 mol % Nb_2O_5; 5.– 10 mol % Nb_2O_5; 6.– Pure Bi_2O_3

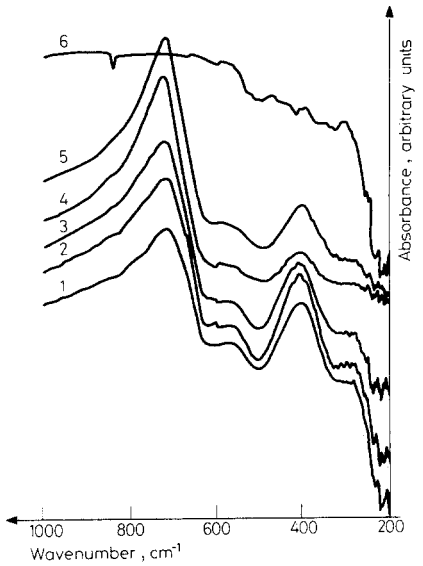

Fig. 2 An illustration for the infrared absorption spectra of pure and Y_2O_3-doped Bi_2O_3 samples. 1.– 2 mol % Y_2O_3; 2.– 4 mol % Y_2O_3; 3.– 6 mol % Y_2O_3; 4.– 8 mol % Y_2O_3; 5.– 10 mol % Y_2O_3; 6.– Pure Bi_2O_3

Table 1 The room temperature characteristic infrared absorption bands and their corresponding energy (eV) for pure and doped Bi_2O_3 samples

Sample	IR bands, cm^{-1}	Corresponding energies, eV
Pure Bi_2O_3	1335(m); 845(w); 500(w, b)	0.171; 0.105; 0.062;
	420(w); 330(w)	0.052; 0.041
2 mol % Y_2O_3	500(m); 290(vw)	0.062; 0.004
4 mol % Y_2O_3	620(w, b); 500(m)	0.077; 0.062
6 mol % Y_2O_3	500(m)	0.062
8 mol % Y_2O_3	620(vw); 490(m)	0.077; 0.061
10 mol % Y_2O_3	490(m)	0.061
2 mol % Nb_2O_5	700(s); 600(s); 560(m);	0.087; 0.074; 0.069;
	520(w); 460(w)	0.064; 0.057
4 mol % Nb_2O_5	690(m); 670(m); 600(s);	0.086; 0.083; 0.074;
	510(w, b); 560(w, b); 415(vw);	0.063; 0.057; 0.051;
	395(vw); 380(vw); 370(vw);	0.049; 0.047; 0.046;
	350(m)	0.043
6 mol % Nb_2O_5	770(vw, b); 690(vw); 670(msh);	0.095; 0.086; 0.083;
	600(s); 515(vw); 500(vw);	0.74; 0.064; 0.062;
	415(vw)	0.051
8 mol % Nb_2O_5	780(wb); 480(mb); 335(vwb)	0.098; 0.060; 0.041
10 mol % Nb_2O_5	780(mb); 490(mb); 330(wb)	0.098; 0.061; 0.041

(s): Strong; (m): Medium; (w): Weak (vw): Very weak; (b): Broad; (vb): Very broad; (sh): Shoulder.

correlated with the higher number of induced lattice imperfections in Nb_2O_5-doped Bi_2O_3, particularly for specimens containing up to 6 mole % Nb_2O_5 (see Fig. 1).

The absence of these clusters usually accompanies cubic solid solution (CSS) formation in both Nb_2O_5 and Y_2O_3-doped Bi_2O_3.

In accordance with Barraclough [15], the absence of absorption bands in the range 900–1100 cm^{-1} for all investigated specimens suggests the absence of metal-oxygen double bonds.

As general trend in common for both specimens, the most intense absorption bands suffer broadening and shift to larger wavelength (lower energy) with increasing molar ratio of the dopant. This could be ascribed to the formation of interaction products vibrating at lower energy levels and/or the decrease of the bond strength in the same direction (see Figs 1 and 2).

Figures 3 and 4 show the room-temperature Cu K_α X-ray diffraction patterns of the $(Bi_2O_3)_{1-x}(Nb_2O_5)$ and $Bi_2O_{31-x}Y_2O_3$ systems, where x ranges from 0.02 up to 0.1, or the ratio of the Nb_2O_5 or Y_2O_3 dopant ranges from 2 up to 10 mol %. When the X-ray results obtained on the two systems were compared with those of ASTM cards Nos. 2–0542, 6–0294 and 6–0312, it was concluded in summary that:

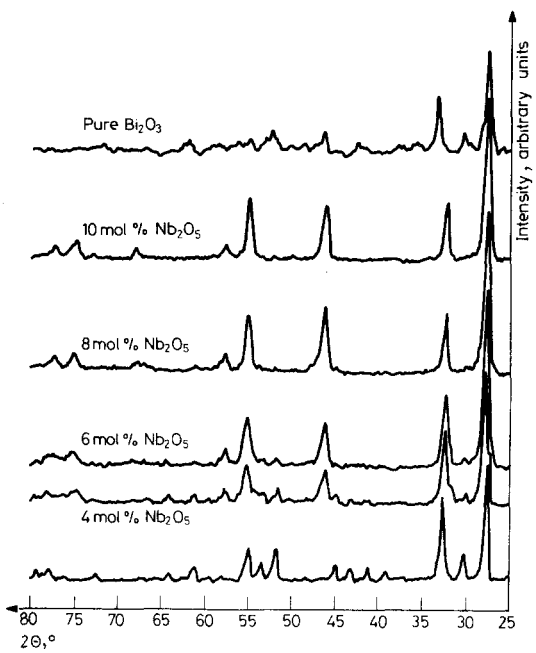

Fig. 3 A diagram showing the X-ray diffraction patterns of pure and Nb_2O_5-doped Bi_2O_3

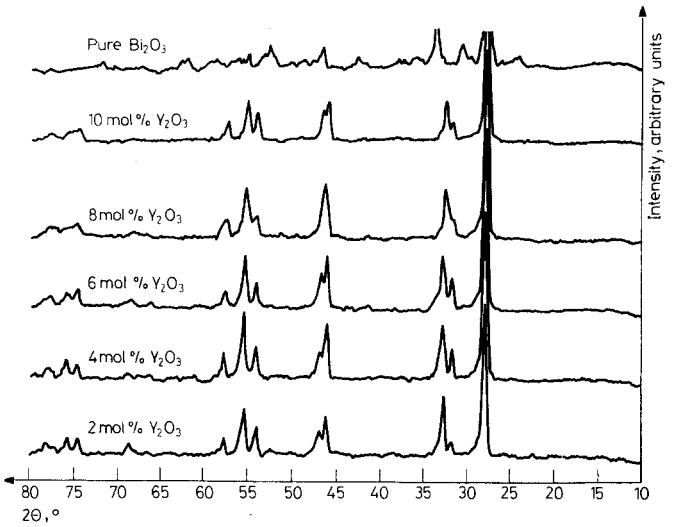

Fig. 4 A representation showing the X-ray diffraction patterns of pure and Y_2O_3-doped Bi_2O_3

1) Pure Bi_2O_3 (α-form) exists in the monoclinic crystal system. 2) The obtained X-ray diffraction patterns of Nb_2O_5-stabilized Bi_2O_3 (Fig. 3) change gradually through monoclinic to mixed phases (monoclinic + cubic) to distorted cubic ending with completely cubic solid solution (CSS) for 8 and 10 mol % Nb_2O_5. However, in the case of Y_2O_3 dopant, the X-ray diffraction pattern (see Fig. 4) suddenly inverts from the monoclinic system to the formed cubic solid solution, even in the first step of Y_2O_3 doping (2 mol %). Thus, in this system (Bi_2O_3–Y_2O_3) perfect solid solution is formed in the entire composition range [16]. This could plausibly be correlated with the fact that Y_2O_3 is a more active mineralizer than Nb_2O_5, including faster stabilization for Bi_2O_3. Furthermore, as a general trend in common, the X-ray diffractograms (Figs 3 and 4) sharpen and show a decrease in numbers as a function of increasing ratios of Nb_2O_5 and Y_2O_3 up to 10 and 8 mol %, respectively. This could be correlated with the increased degree of crystallinity and the decreased lattice imperfections of the formed cubic solid solution in both cases.

The total electrical conductivity of electroded disks was measured to determine the effect of the dopant cation on the electrical properties of the stabilized Bi_2O_3 pellets. Thus, Figs 5 and 6 show the temperature-dependence of the total conductivity for Bi_2O_3 samples containing from 2 to 10 mol % of dissolved Nb_2O_5 and Y_2O_3, respectively. From the latter wo Figures, it can easily be seen that the DC-electrical conductivity is sensitive to structural or phase change. Consequently, any discontinuous change in the DC-electrical conductivity may indicate a change

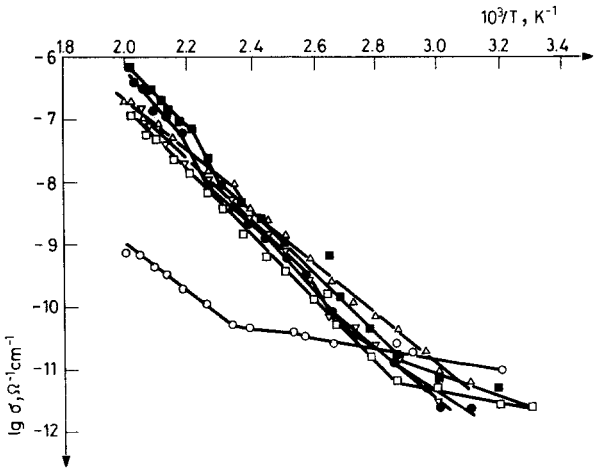

Fig. 5 A plot showing the temperature dependences of electrical conductivity for Nb_2O_5-doped Bi_2O_3. ○ Pure Bi_2O_3; ● 2 mol % Nb_2O_5; △ 4 mol % Nb_2O_5; ▽ 6 mol % Nb_2O_5; □ 8 mol % Nb_2O_5; ■ 10 mol % Nb_2O_5

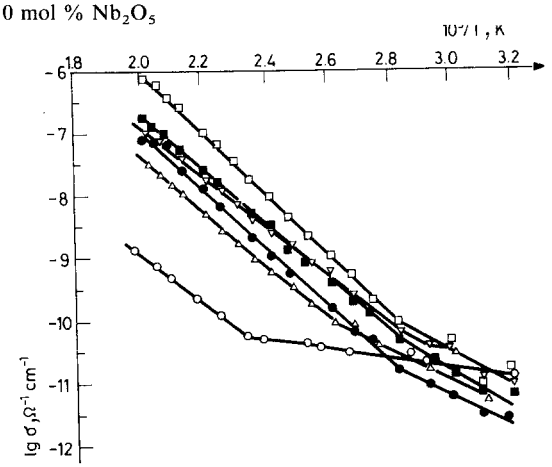

Fig. 6 The temperature dependence of electrical conductivity for Y_2O_3-doped Bi_2O_3. ○ Pure Bi_2O_3; ● 2 mol % Y_2O_3; △ 4 mol % Y_2O_3; ▽ 6 mol % Y_2O_3; □ 8 mol % Y_2O_3; ■ 10 mol % Y_2O_3

in the electronic state, which is critically influenced by the structural and electrical polarization changes. Since there is a positive temperature coefficient of electrical conductivity ($d\delta/dT$) for all curves (see Figs 5 and 6), all the materials investigated are semiconductors. At temperatures above 400 K, the conductivity seems to be principally ionic for all samples. Experimental evidence for this is that values of ΔE_0 (high-temperature activation energy) are twice those of ΔE (activation energy at relatively low temperature, Figs 5 and 6). It was found that the ionic conductivity increases slightly with increasing incorporation of either niobium or yttrium. Such

an increasing ionic conductivity is thought to result from the higher vacancy mobility accompanying the increasing lattice constant, as discussed previously for other materials [17], and/or from the presence of many vacancies. Below 400 K, the conduction mechanism becomes increasingly electronic as the low-temperature extreme is approached. The conductivity varies with temperature according to the well-known relation [18]:

$$\sigma = \sigma_0 \cdot e^{-\frac{\Delta E}{2k} T}$$

where σ is the electrical conductivity at temperature T K, is the pre-exponential constant, ΔE is the activation energy for conduction (= 0.4 × slope in eV), k is the Boltzmann constant and T is the absolute temperature. The ΔE_0 values are calculated to correspond to the activation energies for defect mobilities. From Table 2 and Figs 7 and 8, it is obviously seen that the activation energies ΔE_0 (energy gap E_g, eV) is considerably decreased as a function of the molar ratio of either Nb_2O_5 or Y_2O_3 dopant, reaching constancy. This could be explained by a

Table 2 Log σ at 150 °C and energy gap (E_g) for the investigated samples

Sample		Log σ (150)	E_g, eV
Pure Bi_2O_3		−9.5103	3.40
2% Nb_2O_5	(mol %)	−7.72566	2.63
4% Nb_2O_5	(mol %)	−7.4631	2.91
6% Nb_2O_5	(mol %)	−7.7184	2.09
8% Nb_2O_5	(mol %)	−8.1824	2.17
10% Nb_2O_5	(mol %)	−7.5540	2.17
2% Y_2O_3	(mol %)	−8.0543	2.13
4% Y_2O_3	(mol %)	−7.2480	1.82
6% Y_2O_3	(mol %)	−7.6604	1.71
8% Y_2O_3	(mol %)	−7.0000	1.89
10% Y_2O_3	(mol %)	−7.3145	1.75

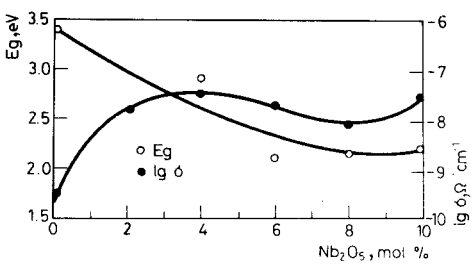

Fig. 7 A diagrammatical representation for the variation of electrical conductivity at 150 °C (log σ 150) and energy gap (Eg) for Nb_2O_5-doped Bi_2O_3

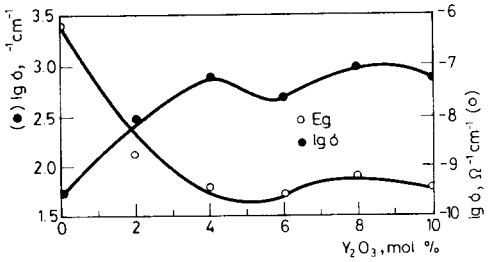

Fig. 8 A schematical representation for the variation of log σ 150 °C and Eg as a function of Y_2O_3 doping of Bi_2O_3. ○ Eg; ● Log σ

decrease in bond strength and increased lattice imperfections, which may lead to defective crystal lattices in the same direction. Another contribution to the increased electrical conductivity and decreased energy gap (E_g) by doping is the dopant-induced non-stoichiometric effect [18]. This evidence is more pronounced for Y_2O_3 dopant than for Nb_2O_5 dopant. This could be attributed to the differences in the vacancy states and ionic radii of the Bi^{3+} and Nb^{5+} cations, leading to easier dissolution and diffusion of Y^{3+} cations in the Bi_2O_3 lattice, facilitating solid solution formation and hence stabilization of Bi_2O_3.

In conclusion, 8 mol % Y_2O_3 and 10 mol % Nb_2O_5 are the optimum compositions for the production of Nb_2O_5 and Y_2O_3-stabilized Bi_2O_3 (both in the cubic SS crystal form) for their useful application as varistors in industry.

References

1 M. Graciet, R. Salman, G. Le Flem, P. Hagenmüller and F. Buchy, Nouv. J. Chim., 1 (1980) 29.

2 G. S. Snow, S. S. White, R. A. Copper and J. R. Armyjo, Am. Ceram. Soc. Bull., 59 (1980) 17.

3 W. D. Kingery, J. B. Vander Santa and R. J. Mitmaura, Am. Ceram. Soc., 62 (1979) 221.

4 D. R. Clarke, J. Appl. Phys., 49 (1978) 2407.

5 H. A. Harving, Z. Anorg. Allg. Chem., 444 (1978) 151.

6 H. A. Harving and J. W. Weenk, Z. Anorg. Allg. Chem., 444 (1978) 167.

7 L. G. Sillen, Ark Kemi, Mineral. Geol., 12 A (1937) 1.

8 G. Gattow and H. Schreeder, Z. Anorg. Allg. Chem., 318 (1962) 176.

9 H. A. Harwing and A. G. Gerards, J. Solid State Chem., 26 (1978) 265.

10 M. Miyayama, S. Katsuta and H. Yanagida, Nippon Kagaku Kaishi 1583 (1981).

11 T. Takahashi, H. Imahara and T. Aroa, J. Appl. Electrochem., 5 (3) (1975) 187.

12 T. Takahashi, T. Esaka and H. Imahara, J. Appl. Electrochem., 7(1) (1977) 31.

13 M. M. Abou-Sekkina, M. A. Ewaida, M. M. F. Sabry and R. M. El-Bahnasawy, Thermochim. Acta, 73 (1984) 131.

14 R. S. Betsch and W. B. White, Spectrochim. Acta, 34 A (1978) 505.

15 G. G. Barraclongh, J. Lewis and R. S. Nyholme, J. Chem. Soc., 3559 (1959).

16 M. H. Lee and W. K. Choo, J. Appl. Phys., 52(9) (1981) 5767.

17 J. R. R. V. Wilhelm and D. S. Howarth, J. Am. Ceramic Bull., 58 (1979) 229.

18 M. M. Abou-Sekkina, J. P. Bonnet, J. C. Grenier, M. Onillon, M. Poucherd and P. Hagemüller, Rev. Chim. Miner., 17 (1980) 431.

Zusammenfassung — Einige Proben von mit Nb_2O_5 und Y_2O_3 gedopten Bi_2O_3 wurden hergestellt und bei 700 °C 3 Stunden gesintert. Von den Proben wurden Röntgendiffraktogramme und IR-Absorptionsspektren aufgenommen und die Temperaturabhängigkeit der elektrischen Gleichstromleitfähigkeit im festen Zustand gemessen. Die erhaltenen Ergebnisse werden diskutiert, zueinander in Beziehung gesetzt und interpretiert. Optimale Zusammensetzungen werden ermittelt und für gedoptes Bi_2O_3 in der Elektronikindustrie empfohlen.

Резюме — Несколько образцов Bi_2O_3, легированных Nb_2O_5 и Y_2O_3, были получены спеканием в течении 3 часов при температуре 700°. Полученные образцы были исследованы методом рентгеновской и инфракрасной спектроскопии, а также измерением температурной зависимости электропроводности. Проведено обсуждение полученных результатов и установлены некоторые корреляции. Найдены оптимальные условия легирования образцов окиси висмута, которые представлены в качестве рекомендаций для электронной промышленности.